ADVANCED MATERIALS INTERFACES
www.advmatinterfaces.de

Nanocontainers for Self-Healing Coatings

*Dmitry Grigoriev, Elena Shchukina, and Dmitry G. Shchukin**

This progress report covers recent achievements in the development of nanocontainers for self-healing corrosion protection coatings. The functionality and design of Layer-by-Layer-assembled, polymer, and inorganic nanocontainers are demonstrated in the coatings for protection of steel and aluminium alloys. The release of the corrosion inhibitors from nanocontainers occurs only when triggered by local pH changes or other internal or external stimuli, which prevents leakage of the corrosion inhibitor out of the coating and increases coating durability. This leads to the self-healing ability of the coating and terminates corrosion propagation.

1. Introduction

Intelligent bulk structures and surfaces modified in order to respond to a specific external stimulus in a defined manner play a significant role in a new generation of smart materials possessing both active and passive functionalities, which enable fine spatial and temporal control over surface properties in three-dimensional space and mimic natural events during materials' exploitation time. Over the past decade, the advances in chemistry, materials science and biotechnology resulted in new classes of potentially active structures for application as components of either smart bulk materials or films. This includes intrinsically active polymers, nanocapsules and nanotubes.[1] The formulation of these structures requires, however, advanced knowledge in nanomaterials with the potential to meet specific industrial requirements. This is very challenging task facing us with multiple requirements depending on the specific application, such as efficient encapsulation of molecules, retention of their self-healing or other activity during the encapsulation process and storage, protection of encapsulated active agents against degradation in the bulk structures and controlled release over extended time periods at defined target sites.

Dr. D. Grigoriev
Fraunhofer Institute for Applied Polymer Research IAP
Geiselbergstrasse 69, 14476 Potsdam-Golm, Germany
Dr. E. Shchukina, Prof. D. G. Shchukin
Stephenson Institute for Renewable Energy
Chadwick Building, Peach Street, L69 7ZF Liverpool, UK
E-mail: d.shchukin@liverpool.ac.uk

DOI: 10.1002/admi.201600318

Mimicking the concept of the natural feedback active systems in the field of synthetic coatings and surfaces provides broad avenue for the development of "smart" coatings with stimuli-responsive behavior. Self-healing coatings undergo a change in response to an external stimulus in a defined manner to enhance the system performance. These coatings are of great scientific and technological importance, as they can be applied in various fields such as medicine, biotechnology or material science. Surface polymer films and capsules can enable fine spatial and temporal control over surface properties in three-dimensional space and better mimic natural events. To provide sustained or immediate release of the functional material on demand, the active part of the coating has to be incorporated into a passive matrix or form a layered structure together with the passive matrix.

Recent developments in surface science and technology provide modern engineering concepts for fabrication of active feedback coatings through the integration of nanoscale layers (carriers) loaded with active compounds (e.g., inhibitor, lubricant, drug, vitamin) into existing "classical" films thus designing completely new coating systems of the "passive" host – "active" guest structure.[2] For example, active corrosion protection aims to restore material properties (functionality) if the passive coating matrix is penetrated and corrosive species come into contact with the substrate. In addition, the partial recovery of the main functionality of a material can also be considered as self-healing ability.[3] The main function of anticorrosion coatings is protection of the underlying metallic substrate against environmentally induced corrosion attacks. Thus, it is not obligatory to recuperate all properties of the film; only the protection of the substrate has to be guaranteed. Consequently, the coatings have to release the active and repairing material within short time after changes in the coating's integrity (**Figure 1**).

One of the main approaches for self-healing coatings is nanocontainers employed for loading of active agents with shell possessing controlled permeability specific to several triggers.[5] The use of the term "nanocontainers" was introduced to distinguish them from "capsules" because nanocontainers have more broad structure and properties than common capsules for drug delivery. Being uniformly distributed in the passive matrix, these nanocontainers keep the active material in "trapped" state avoiding undesirable interaction between the active component and the matrix as well as spontaneous leakage. If the local environment undergoes changes or the coating is affected by an outer impact, the nanocontainers respond to this stimulus and release encapsulated active material.

Designing functional micro- and nanocontainers in the size range of 20 nm to 50 µm is of high interest in various research

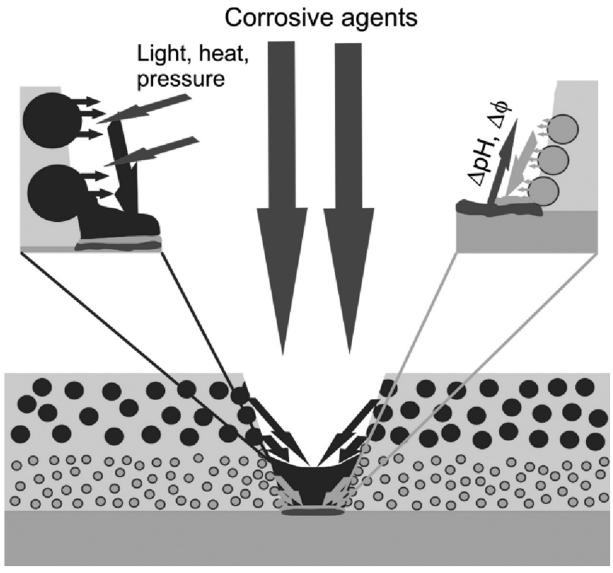

Figure 1. Schematic representation of the nanocapsule-based self-healing coatings. Reproduced with permission.[4]

areas such as biotechnology, medicine, cosmetic, catalysis and functional coatings. In general, research on nanocontainer formation and loading requires the ability to form a nanocontainer shell, which should be stable, permeable to release/upload materials and should also possess other desired functionalities (magnetic, catalytic, conductive, targeting, etc.). One has to combine several properties in the shell structure and composition. There are several approaches demonstrated so far for the design of nanocontainer systems: (1) polymer containers,[6] (2) polymer or glass fibres,[7] (3) nanocontainers with polyelectrolyte shell,[4] layered double hydroxides and mesoporous inorganic materials[8] and, finally, design of the coatings by Layer-by-Layer assembly (LbL) employing polyelectrolyte multilayers.[9] All of the mentioned methods have specific advantages and drawbacks concerning the upscaling possibility, performance and feasibility to employ different active materials. Here, we make a survey of the pros and cons of the nanocontainers of different nature which were tested for application in self-healing coatings.

2. Nanocontainers with Layer-by-Layer Assembled Shell

The Layer-by-Layer technology was presented in 1990s by Decher and others.[10] This technique is very simple and based on the iterative adsorption of oppositely charged molecules or nanoparticles on a flat surface or template particle. In most cases, the technique employs electrostatic forces between oppositely charged polymers and surfaces.[11] However, other mechanisms of film formation can be employed: hydrogen bonding for biomedical applications (most of these multilayers can be disassembled under physiological conditions),[12] covalent bonding,[13] base-pair interactions,[14] guest-host interactions,[15] hydrophobic interactions[16] or biological recognition.[17]

The use of the LbL technique to prepare structured films offers many attractive possibilities. The method allows control over the composition and thickness of the multilayers (e.g., by control over the number of layers deposited) resulting in nanometer-scaled films. A wide variety of polyelectrolytes, both synthetic and natural, can be used in LbL assembly. In addition, almost any charged material, such as nucleic acids,[18] peptides,[19] enzymes,[20] polysaccharides,[21] lipids[22] and also particulate structures such as viruses[23] and a wide variety of nanoparticles[24] can be incorporated into LbL assemblies.

The main principles of LbL deposition on colloidal particles[25] are similar to those for planar surfaces: the concept of capsule formation involves coating of a colloidal template followed by decomposition of the sacrificial core leading to the formation of hollow structures similar to the templates in terms of size and shape.

Dr. Dmitry Grigoriev received his PhD in Physical Chemistry at the University of Saint Petersburg, Russia and since 1996 worked as postdoctoral fellow and further as researcher at Max-Planck-Institute of Colloids and Interfaces. Since 2007, he has been involved in the development of various techniques and systems for the micro- and nanoencapsulation. From February 2016, Dr. Grigoriev is a project leader at Fraunhofer Institute of Applied Polymer Research IAP.

Dr. Elena Shchukina received PhD in Organic Chemistry at the Belarussian Academy of Sciences, Belarus. She has gained experience in organic chemistry working in different industries. Since 2015, she is project leader in Stephenson Institute for Renewable Energy, University of Liverpool.

Prof. Dmitry Shchukin was a group leader at the Department of Interfaces, Max Planck Institute of Colloids and Interfaces, Potsdam, Germany, in 2007–2013. He obtained his PhD (2002) in physical chemistry. Currently, he is Professor in Chemistry, Stephenson Institute for Renewable Energy, University of Liverpool.

As depicted in **Figure 2**, the core can be dissolved after applying LbL layers yielding hollow LbL capsules. The ability of precise manipulation of capsule structures enables the tailoring of permeability, loading and release, mechanical properties as well as other functionalities of the capsules.

The shell of the polyelectrolyte capsules is semipermeable and sensitive to a variety of physical and chemical conditions of the surrounding media which might dramatically influence the structure of polyelectrolyte complexes and permeability of the capsules. **Table 1** represents an overview of the different triggers influencing permeability of polyelectrolyte capsules. In addition to well-characterised influence of pH, solvents, ionic strength and temperature on the capsule permeability, the other external factors can control it: external light, magnetic field, ultrasound, oxidation/reduction and enzymatic degradation.

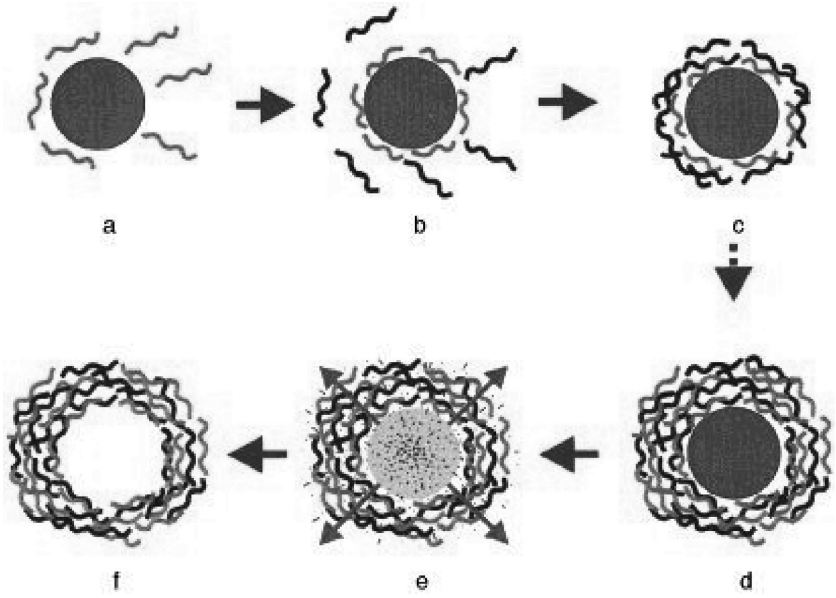

Figure 2. Schematic illustration of the polyelectrolyte capsule formation. a–d) Stepwise polyelectrolyte LbL assembly; e–f) decomposition of template core resulting in polyelectrolyte hollow capsules. Reproduced with permission.[25]

First successful application of the Layer-by-Layer assembly for self-healing anticorrosion coatings was demonstrated in 2006 on the example of silica nanoparticles with LbL assembled shell containing corrosion inhibitors which were impregnated into ZrO_x-SiO_x hybrid sol-gel coating.[34] As nanocontainers, 70 nm SiO_2 particles coated with poly(ethylene imine)/poly(styrene sulfonate) (PEI/PSS) polyelectrolyte layers were employed. The inhibitor, benzotriazole, was entrapped within the polyelectrolyte multilayers during the LbL-assembly step; its release was initiated by pH changes during corrosion of the aluminum alloy.

The average diameter of the nanocontainers obtained from the light-scattering measurements increases with the layer number. For the first PEI and PSS monolayers, the increment is about 8 nm per layer. Benzotriazole layers increase the size of the nanocontainers by a smaller ca. 4 nm step which confirms the electrophoretic mobility data for the lower adsorption efficiency of benzotriazole as compared with the polyelectrolytes. Growth of the average diameter of the nanocontainer unambiguously proves LbL assembly of the polyelectrolytes and the inhibitor on the surface of the SiO_2 nanoparticles.[35] The scanning vibrating electrode technique (SVET) was employed to prove the self-healing ability of nanocomposite coatings by mapping the distribution of cathodic and anodic currents along the surface. Defects of about 200 µm in diameter were formed on the sol–gel pre-treated AA2024 surface, as shown in **Figure 3**. A high cathodic current density appears immediately in the origin of the defect when the undoped coating is immersed in 0.05 M NaCl, revealing well-defined corrosion activity. The defects remain active during tests (Figure 3c,e, and g). The sample coated with sol-gel film doped with nanocontainers behaves completely differently. During the first 10 h, there are no remarkable currents in the defect zone (Figure 3d). Cathodic current appears only after about 24 h. However, 2 h after the activity started, effective suppression of corrosion takes place to decrease the local current density (Figure 3h). Cathodic activity in the location of the defects becomes almost undetectable again after 48 h of continuous immersion. This effective suppression of the corrosion activity at a relatively large

Table 1. Release properties of polyelectrolyte capsules.

Factor	Release characteristics	Ref.
Local changes of pH	Capsules can be opened/closed depending on pH value at all pH range (0–14). Applicable only for capsules with weak polyelectrolytes in the shell	[26]
Local changes of ionic strength	Increase of the ionic strength of solution leads to the capsule opening. Applicable for all polyelectrolyte capsules	[26]
Solvent changes	Unpolar solvents damage integrity of polyelectrolyte shell and open capsules	[27]
Temperature	Temperature increase leads to the capsule closing. Applicable for capsules with strong polyelectrolyte in the shell	[28]
Light	Irradiation leads to the capsule opening. Applicable for capsules with light-sensitive elements in the shell	[29]
Magnetic field	Magnetic treatment opens capsules. Applicable for capsules with magnetic particles in the shell	[30]
Ultrasound	Ultrasonic treatment leads to irreversible capsule opening. Applicable for capsules with nanoparticles in the shell	[31]
Redox treatment	Oxidation/reduction of the capsule shell can lead to the capsule opening. Applicable for capsules with redox materials in the shell (conductive polymers)	[32]
Enzymatic degradation	Enzymatic treatment irreversibly opens capsules with biodegradable components in the shell	[33]

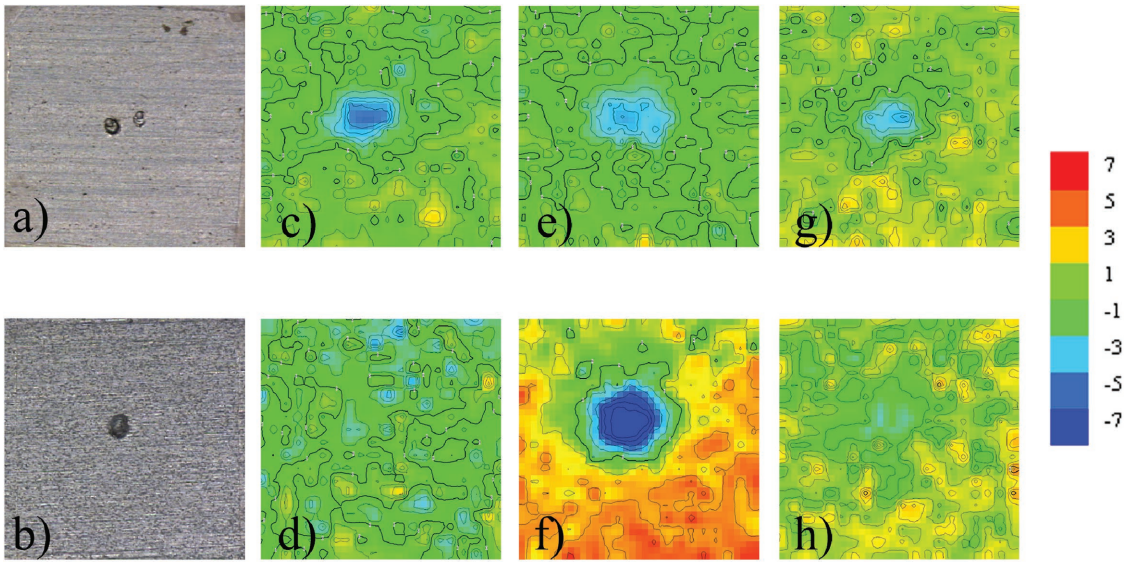

Figure 3. SVET maps of the ionic currents measured above the surface of artificially defected aluminium alloy (a,b) coated with undoped silica-zirconia sol-gel film (c,e,g) and film with inhibitor-loaded nanocontainers (d,f,h). The maps were obtained 5 (c,d), 24 (e,f) and 26 (g,h) hours after defect formation. Scale units: μA cm^{-2}. Reproduced with permission.[34]

artificial defect formed in the coating system clearly proves the self-healing ability of the hybrid pretreatment films doped with nanocontainers.

Introduction of the inhibitor in the form of nanocontainers instead of the direct addition to the sol-gel matrix prevents the interaction of the benzotriazole with components of the coating which negatively influences the barrier properties of the hybrid film and lead to the deactivation of the corrosion inhibitor.

Next stage in the application of LbL assembly for self-healing coatings is the formation of the core-shell type containers with oil core and polymer/polyelectrolyte shell. Several groups employed LbL technology to fabricate stable oil-in-water emulsions with a high monodispersity (depending on the size of the oil core used in capsule preparation) and free of surfactant.[36] A usual preparation method for LbL coated emulsion carriers involves several steps (**Figure 4**).[37] To stabilize the dispersed phase of initial emulsion, the oil phase (dodecane) was doped by small amount of cationic surfactant dioctadecyldimethylammonium bromide (DODAB). The colloidal stability of initial emulsion was achieved due to concentrated monolayer of strongly positively charged DODAB (z-potential was about +90 mV) at the surface of each droplet. Then, the subsequent LbL deposition was performed from concentrated aqueous salt-free solutions of polyelectrolytes. The further repetition of the alternating adsorption steps leads to the formation of containers with desired shell thickness depending on the particular demand.

The improved stability of the LbL coated emulsions to droplet aggregation can be attributed to the ability of the multilayered interfaces to increase the repulsive colloidal interactions between the droplets (e.g., electrostatic and steric) and to increase the resistance of the interfacial membrane to rupture.

Pickering emulsions (or colloidosomes) are emulsions stabilized by solid particles localized at the oil-water interface. Since particle stabilized droplets resemble core shell architectures, they have a high potential to be applied in the field of active molecule encapsulation. The application of the Layer-by-Layer assembly approach for Pickering emulsions not only stabilizes the emulsion particles due to the electrostatic repulsion,

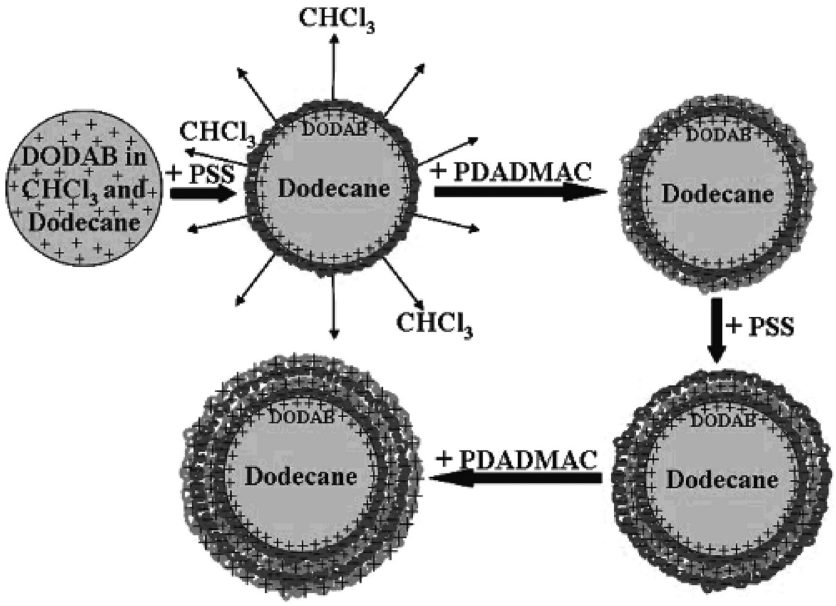

Figure 4. Schematic representation of several steps during LbL polyelectrolyte emulsion encapsulation. Reproduced with permission.[37] Copyright 2008, ACS.

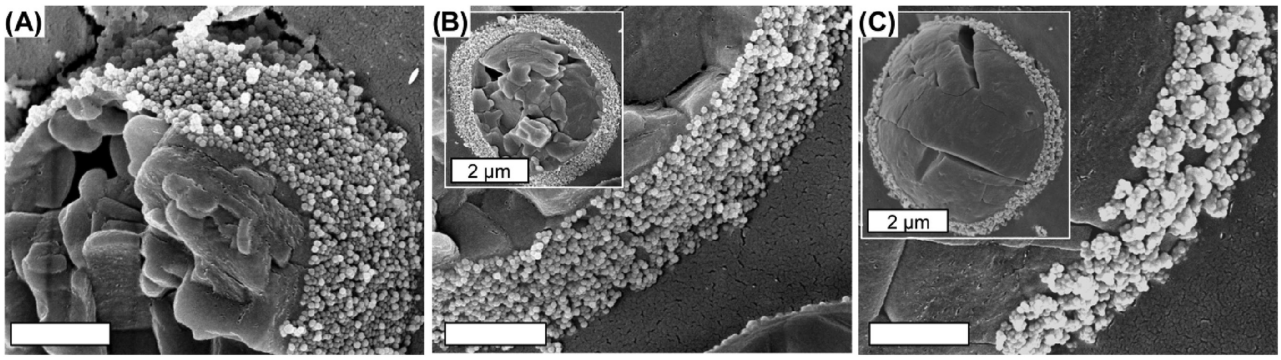

Figure 5. Cryo SEM images of dodecane droplets stabilized with silica-poly(allylamine hydrochloride) particles. Corresponding pH values of emulsions are (a) 8.5, (b) 9.1, and (c) 9.8. Length of unlabeled scale bars equals 500 nm. Reproduced with permission.[38] Copyright 2011, ACS.

but also closes the interstitial pores of the emulsion nanoparticulated shell thus providing its controlled permeability and release of the materials dissolved in the oil core.

The affinity of weak polyelectrolyte coated oxide particles to the oil-water interface can be controlled by the degree of dissociation and the thickness of the weak polyelectrolyte layer.[38] Thereby the oil in water (o/w) emulsification ability of the particles can be enabled. To demonstrate this, weak polyacid poly(methacrylic acid sodium salt) and the weak polybase poly(allylamine hydrochloride) were selected for the surface modification of oppositely charged alumina and silica colloids. To prepare the emulsion samples, first the aqueous components were mixed and, depending on the pH, colloidal or gelated suspensions of nanoparticles in water were obtained. Highly stable emulsions can be obtained when the degree of dissociation of the weak polyelectrolyte is below 80%. Cryo-SEM visualization shows that the regularity of the densely packed particles on the oil-water interface correlates with the degree of dissociation of the corresponding polyelectrolyte (**Figure 5**).

Silica- poly(allylamine hydrochloride) particles arrange themselves in a monolayer, which partially consists of some aggregates below pH 9.2. Above this pH value, flocculation of particles takes place; consequentially, the droplet shell consists almost entirely of particle aggregates. Less pronounced but still established is the fact that for the same emulsion pH, particles with thicker polyelectrolyte coatings are capable of creating smaller droplets. The average droplet size reaches a minimum between pH 4.5 and 5.5 ($0.15<R<0.45$). The nanocontainers were well dispersed in the coating. SVET measurements indicated a decreased rate of corrosion in scratches of coatings doped with 8-hydroxyquinoline loaded SiO_2 Pickering emulsion. For all samples, maximum current densities different from zero were observed immediately after immersion in 0.1 M NaCl indicating the formation of an anodic area in the scratch. However, addition of 20 wt% 8-hydroxyquinoline loaded SiO_2 Pickering emulsion to the coating suppressed corrosion after 12 h of immersion in 0.1 M NaCl. Another demonstration of the application of Pickering emulsion for self-healing coatings was shown for the shell made of lignin nanoparticules with encapsulated isophorone diisocyanate as healing agent.[39]

In general, nanocontainers for self-healing coatings made by LbL assembly approach have one big advantage – the possibility to tailor functionality of the shell. Besides pH-responsive release of encapsulated inhibitor, the release triggered by UV or IR light was demonstrated for successive localized healing with either TiO_2 or Ag nanoparticles in the shell [skorb]. The drawback, however, is the poor mechanic stability of the shell which makes difficult to stabilize LbL nanocontainer integrity in the dried commercial coatings.

3. Nanocontainers with Polymer Shell

More rigid core-shell type nanocontainers can be prepared by polymerization methods at the oil-water interface of emulsion droplets. The shell, in this case, has no so well controlled structure like for LbL assembled shells, but it is thicker and can be responsive to the local changes of the pH.

Urea-formaldehyde microcapsules filled with linseed oil were used for the healing of cracks in an epoxy coating.[40] Microcapsules were synthesized by in situ polymerization in o/w emulsion. Initially, fully water-compatible urea and formaldehyde react in continuous aqueous medium to form poly(urea-formaldehyde). As molecular weight of this polymer increases the fraction of polar groups gradually decreases till the polymer molecules become hydrophobic and get deposited on the surface of o/w-emulsion droplets. Obtained microcapsules were then incorporated into epoxy coating. The encapsulated linseed oil was released by the coating crack and filled the crack in a coating matrix. Oxidation of linseed oil by atmospheric oxygen led to the formation of continuous film inside the crack. Similar containers were developed by interfacial polymerization of commercial methylene diphenyl diisocyanate and polyamidoamine dendrimer.[41] Spherical with some irregular shape microcapsules were observed with average diameter from 20 to 270 μm at different agitation rates (3000–8000 rpm). Microcapsule size decreases with increasing agitation rate applied during the emulsion step. The results from the corrosion immersion tests in salt solution (5% NaOH) clearly demonstrated that coating with increasing microcapsule content from 2 to 5% revealed decreasing order of corrosion and blistering at the scribed lines after 120 h of immersion. In contrast, rapid corrosion was seen in the control specimen within 24 h and exhibited severe corrosion after 120 h, most prevalently within the scribed area also extending rusting across the substrate surface.

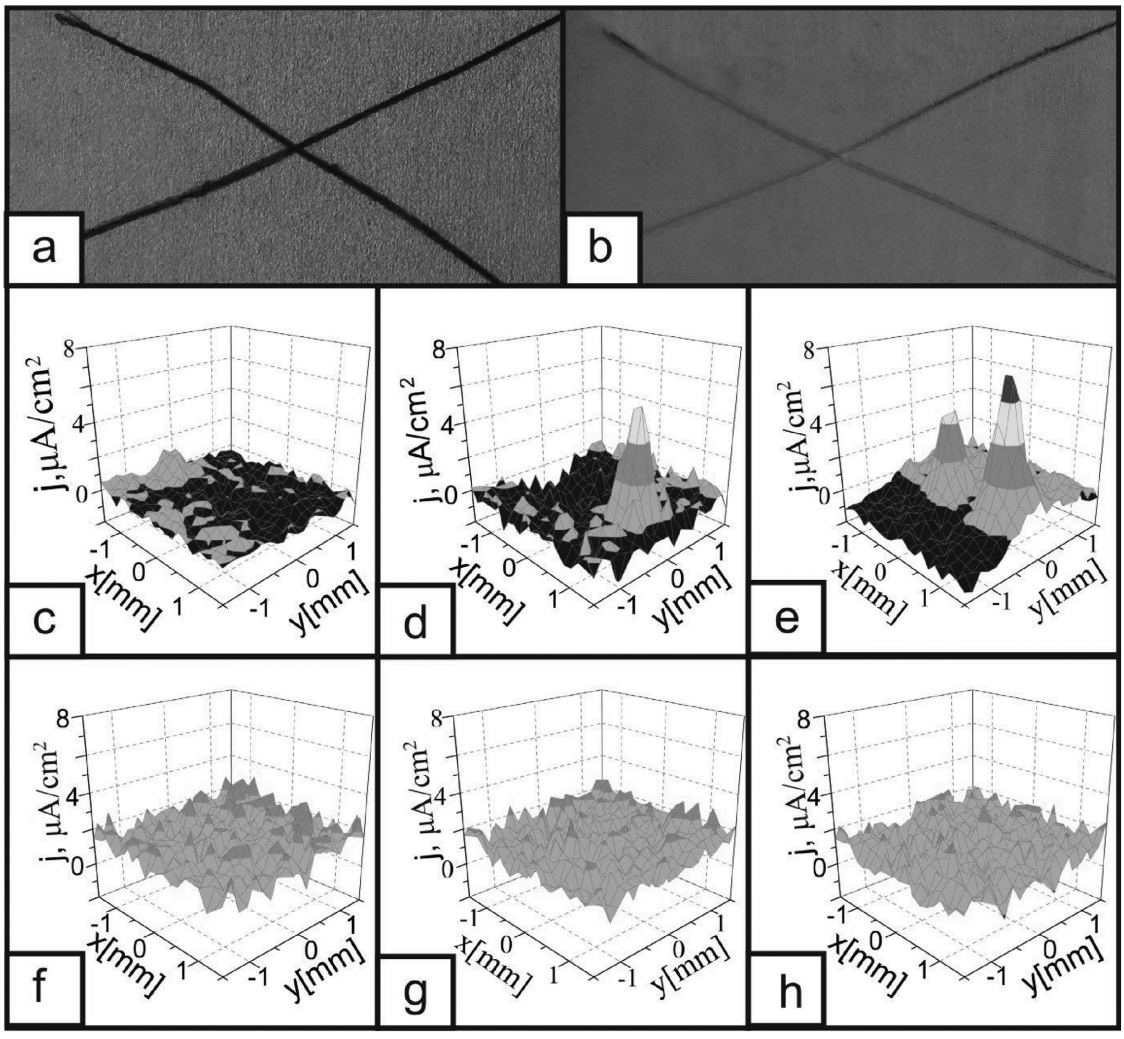

Figure 6. Optical images after 12 h of immersion in 0.1 M NaCl solution of (a) aluminum alloy plates covered with the standard epoxy coating (control sample), (b) self-healing coating consisting of standard epoxy coating and 6%. microcontainers loaded with mixture of alkoxysilanes. c–h) SVET current density maps after 0 (c,f), 1 (d,g) and 12 (e,h) hours of immersion in 0.1 M NaCl for control coating (c–e) and self-healing coating (f–h). Reproduced with permission.[42] Copyright 2011, RSC.

Depending on the application purpose, encapsulated oil can also contain either water-repelling agent (alokoxysilane) forming dewetted spot around the damaged site or sealant covering this site with the protective polymeric film.[42] Appropriate protection of the substrate at the damaged site is achieved by the synergetic combination of the passivation effect of the resulting film with its water-repelling properties. A humid or aqueous environment is one of the key preconditions for the corrosion onset; therefore minimization of its contact with the substrate is important for the successful corrosion protection. Creation of non-wetting conditions prevents the contact of water (and dissolved ionic species) with the substrate surface leading to better protection. Hydrophobic compounds with ability to be bound covalently to the substrate under protection are used as active encapsulated agents. The visual corrosion test confirmed the effectiveness of the proposed self-healing system (**Figure 6**). All control samples showed the corrosion onset already 6 hours after immersion in 0.1 M NaCl solution (the process starts with the blackening of the defect surface followed by the appearance of a white fluffy precipitate within the groove of the scratched regions). In contrast, the self-healing samples showed no visual evidence of corrosion even 3 days after exposure. Liquid corrosion inhibitor (2-methylbenzothiazole) was encapsulated into similar polymer capsules for self-healing protective coatings.[43] The capsules with a mean diameter of 5 μm and inhibitor content around 50 wt% were homogeneously introduced into a conventional two-component waterborne epoxy primer of 30 μm thickness. The results of the electrochemical impedance spectroscopy measurements show that the polymeric coating system containing capsules loaded with 2-methylbenzothiazole has better anticorrosion protection than the original unmodified coating. The improvement can be attributed to both the presence of the inhibiting species as well as the improvement of the barrier properties of the coating. Cinnamide moiety containing polydimethylsiloxane shells (CA-PDMS) was prepared and used as a healing agent.[44] CA-PDMS was microencapsulated with a

urea-formaldehyde polymer shell. Upon photo-irradiation, CA-PDMS generates viscoelastic substances which have intrinsic recoating (or self-healing) capability when scribed with a cutter blade. The prepared microcapsules were integrated into commercial enamel paint to create a self-healing coating.

Nanocapsules filled by dicyclopentadiene as self-healing agent were synthesized using ultrasonic treatment for the preparation of initial o/w-emulsions.[47] Up to 2 v/v% of these capsules can be dispersed in an epoxy matrix leading to the slight decrease of its tensile strength accompanied by a significant increase in fracture toughness. Fracture toughness increase up to 59% was found for a capsule volume fraction of 0.015. Copper/liquid microcapsule composite coatings with polyvinyl alcohol, gelatin or methyl cellulose as shell materials were prepared by electrodeposition.[48] The influence of shell materials on the corrosion resistance of the composite coatings in 0.1 M H_2SO_4 was investigated by means of electrochemical techniques, scanning electron microscopy and energy dispersion spectrometry. The results show that the participation of microcapsules enhances the corrosion resistance of the composite coatings compared with the traditional copper layer. The release from microcapsules was triggered by changes of electrochemical potential of the copper coating. Gelatin and methyl cellulose as the shell materials of microcapsules are easy to release quickly in the composite coating.

The bilayer nanocapsules, which have an intermediate hydrophilic shell and a hydrophobic outermost shell, were capable of loading amine-type corrosion inhibitors by interaction of the carboxylic acid in the core polymer and the amines.[49] The amines with high water solubility were more efficient in both swelling and encapsulation than the amines with low water solubility. The strongly basic amines were more effectively encapsulated due to higher dissociation activity than the weak bases. Among six amines used in the study, 5-amino-1-pentanol, diethanolamine and triethanolamine exhibited self-healing anticorrosion performance with recovering coating resistance. The corrosion resistance of the coating film gradually decreased and then increased via the self-healing protection of the amines released from the nanocapsules. On the other hand, ethanolamine, propylamine and dipropylamine exhibited a rapid drop in the coating resistance, and the resistance continued to decrease with- out self-recovery.

Nanocontainers with organic (polymer) shell can be effectively applied for water-borne polymer coatings used for protection of the aluminium alloys and steel. These coatings have mild curing conditions (in most cases can be simply dried in open air). The advantages of such core-shell containers are high loading capacity (since all inner volume can be filled with liquid inhibitor) and possibility to design permeability properties of the shell. However, the nature of the nanocontainers limits their application. They can hardly be applied for oil-borne coating because of the potential solubility of the shell in organic solvent of the coating formulation. They cannot withstand harsh curing conditions (high temperatures and pressure). Polymer shell is stable up to 120–150°C and the inner cargo undergoes thermal expansion. Therefore, nanocontainers of other nature should be explored to attain self-healing functionality for all types of the coatings.

4. Inorganic Nanocontainers

An interesting alternative to the organic core-shell nanocontainers described above is mesoporous inorganic materials, especially silica. Mesoporous silica particles are inert towards the corrosion inhibitors and UV light, comparing to mesoporous TiO_2 and ZrO_2, and have large pore volume (≈ 1 mL g^{-1}) and surface area (≈ 1000 m^2 g^{-1}) which makes possible to incorporate up to 40 wt% of inhibitor.[45] Inhibitor-loaded silica nanoparticles enhance both passive and active functionalities of the anticorrosive coatings. On one hand, the coating barrier properties are improved by reinforcement of the coating matrix due to introduction of mechanically stable, robust silica nanoparticles. This is an advance of silica nanocontainers because the incorporation of polymer-based nanocontainers usually makes the coating more brittle. On the other hand, the large amount of encapsulated inhibitor and its controlled, local release provide superior active corrosion inhibition. Additionally, the outer surface of inhibitor-loaded silica nanoparticles can be functionalized with octyl groups for better dispersibility in the oil-based coatings.[50]

Dispersion of mesoporous silica nanocontainers loaded with the 20 wt% non-toxic corrosion inhibitor 2-mercaptobenzothiazole (MBT) in a hybrid sol-gel (SiO_x/ZrO_x) layer resulted in the substantial enhancement of the corrosion protection activity.[45] The following concentrations of MBT-loaded silica nanocontainers dispersed homogeneously everywhere in the cured coatings were studied: 0.04, 0.1, 0.2, 0.5, 0.7, 0.8, and 1.7 wt% (**Figure 7**).

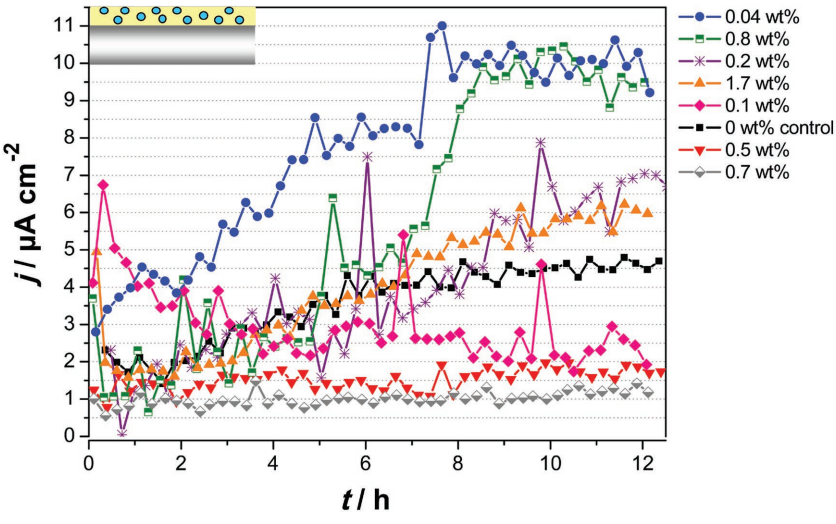

Figure 7. Maximum anodic current densities detected with SVET over the scanned scratched area during 12 hours immersion in 0.1 M NaCl. Results for coating samples containing different MBT-loaded SiO_2 concentrations are shown. Reproduced with permission.[45] Copyright 2012, ACS.

ADVANCED MATERIALS INTERFACES
www.advmatinterfaces.de

Materials Views
www.MaterialsViews.com

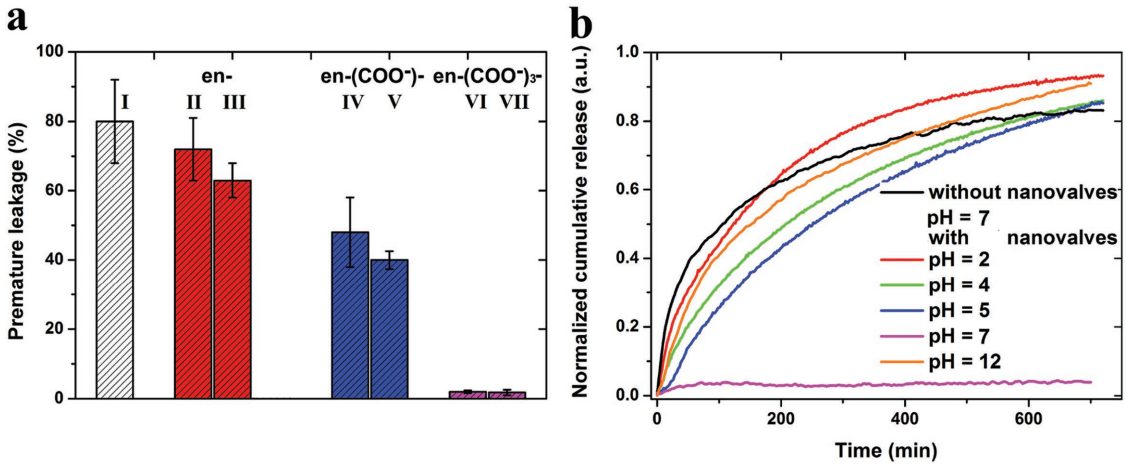

Figure 8. a) The premature leakage of benzotriazole (BTA) from I (native MCM-41), II (FSNs 1, en-SiO_2 with organic content 0.22 mmol g^{-1}), III (FSNs 2, en-SiO_2 with organic content 0.7 mmol g^{-1}), IV (FSNs 3, with organic content 0.26 mmol g^{-1}), V (FSNs 4, en-(COO^-)-SiO_2 with organic content 0.78 mmol g^{-1}), VI (FSNs 5, en-$(COO^-)_3$-SiO_2 with organic content 0.23 mmol g^{-1}), VII (FSNs 6, en-$(COO^-)_3$-SiO_2 with organic content 0.68 mmol g^{-1}) with Co-carbonate nanovalves. The data have been normalized by effective release capacity. d) Release profiles of BTA from the Co-carbonate loaded FSNs 5. Reproduced with permission.[46] Copyright 2015, ACS.

The coating samples were scratched in order to accelerate the corrosion process and assess their active anti-corrosive properties. In the SVET maps this process is expressed as a single positive peak with a constant position over the measurement duration, indicating one defined corrosion site being the anode.

A distinct corrosion propagation expressed by the high values of current density (> 5 μA cm^{-2}) were seen for samples with too high (0.8–1.7 wt%) and too low (0.04–0.2 wt%) MBT-loaded SiO_2 concentrations. These samples reached current densities above the nanocontainer-free suggesting an unsatisfactory active corrosion protection due to an insufficient inhibitor quantity in the coating systems with low MBT-loaded SiO_2 concentrations. In the case of too high MBT-loaded SiO_2 concentrations the bad anti-corrosive properties of the coatings can be explained by deterioration of the passive layer due to microdefects introduced by the embedded nanocontainers. Thus, according to the SVET study, a concentration window in which the corrosion process successfully inhibited was defined to be between 0.5 and 0.7 wt% MBT-loaded SiO_2 incorporated in a single sol-gel layer in direct contact with the metal surface. The SVET results were also supported by the SEM micrographs depicting the scratched area after completing the SVET test.

Despite demonstrated high efficiency of mesoporous silica as nanocontainers for self-healing coatings, the open structure of the pores can still provoke premature leakage of the encapsulated inhibitor. Therefore, the next stage in the development of silica nanocontainers requested the mechanism for controlled opening/closing of the pores on molecular level. This was achieved by organosilyl-functionalization of mesoporous silica nanoparticles with ethylenediamine (en), en-4-oxo-2-butenoic acid salt (en-COO^-) and en-triacetate (en-$(COO^-)_3$) with higher and lower organic content.[46] The cobalt carbonate nanovalves are based on all modified silica nanoparticles (FSNs), according to the method reported by us.[35] Co^{2+} can form a stable complex with iminodiacetic acid with 10^7 order of magnitude formation constant, while the one for Co-carboxylate complexes is always below 1.[51] Co-capped loaded FSNs 5 (VI in **Figure 8**a) lead to the best performance in lowering leakage to 2%. For FSNs 4, a notable leakage of inhibitor at 40% was detected, indicating that even the high dose of en-(COO^-) groups cannot stabilize cobalt basic carbonates as nanovalves. For the other capped containers except FSNs 6 the premature leakages are all above 60% of the loaded amount. Figure 8b confirms the negligible premature leakage of capped loaded FSNs 5 with a flat baseline at neutral environment. Furthermore, lowering pH value helps to accelerate the release of BTA. At the same time, increasing the pH value to 12 was found to stimulate the release of inhibitor as well.

Nanovalve-based pH sensitive nanocontainers are especially suitable for responsive anticorrosion effects, because they provide rapid inhibitor release and protection in response to acidic as well as basic microenvironment. The detected anodic current densities (SVET) as a function of time for the samples coated with doped and non-doped organic coatings are shown in **Figure 9**a. Except the pure epoxy coating, other samples exhibit obvious corrosion resistance and self-healing ability. All the anodic current densities were effectively suppressed at around 2 μA cm^{-2}. This behavior can be attributed to enough inhibitor concentration near the artificial defect. However, after putting the freshly scratched samples in a flowing artificial seawater environment for 1 hour to remove free or leaked inhibitors the coatings containing free BTA and capped loaded FSNs 2 and 4 lost ability of effective self-healing (Figure 9b). The one hosting capped loaded FSNs 5, on the contrary, still maintained the suppression of anodic current. This constantly effective self-healing suggests that the inhibitor can be well preserved in capped FSNs 5 and released when the local pH value is shifted. So, the en-$(COO^-)_3$-type functionalization of mesoporous silica nanocontainers with organic content of 0.23 mmol g^{-1} was shown to be the best nanovalve for anticorrosive nanocontainers.

Second type of highly potential inorganic nanocontainers is the industrially mined, viable and inexpensive halloysite nanotubes. Halloysites are two-layered aluminosilicates with hollow tubular structure. Their size varies within 1–15 μm of length

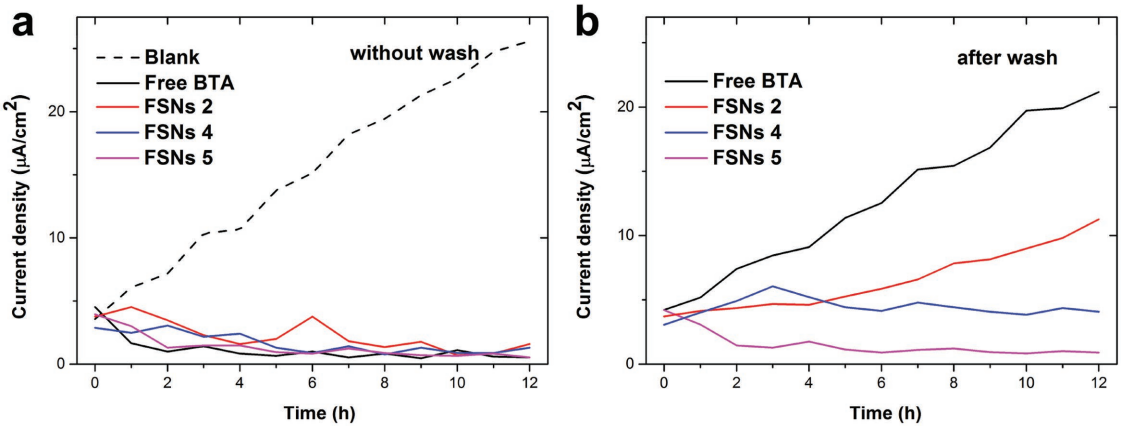

Figure 9. Maximum anodic currents detected with SVET over the scanned scratched area during 12 h immersion period in 0.1 M NaCl. Results are shown for samples coated with an epoxy coating containing nothing, free inhibitor, capped loaded FSNs 2, FSNs 4 and FSNs 5. The measurement was conducted (a) without and (b) after pre-wash with a flowing artificial seawater environment for 1 hour to remove free or leaked inhibitors. Reproduced with permission.[46] Copyright 2015, ACS.

and 10–150 nm of lumen inner diameter. Inner halloysite lumen can reach loading capacity for corrosion inhibitors up to 20 wt% depending on the deposit.[52] Additional selective etching of the alumina inside halloysite lumen with sulfuric acid increases capacity by 2–3 times.[53]

The typical procedure of the loading of halloysite nanotubes is as follows.[54] Halloysites are mixed with the solvent possessing high solubility of desired corrosion inhibitor and low temperature boiling point (e.g., acetone, ethanol). Then, the vial containing solution is placed in a desiccator under vacuum which deaerates the halloysite lumen. The vacuum treatment is followed by washing and centrifugation. This procedure can be repeated several times. On the final stage, halloysites are removed from centrifuge tube and dried.

Embedding of the inhibitor-loaded halloysites into the coating requires intensive mixing of the dried halloysites with coating formulation using high-speed stirrers, UltraTurrex or ultrasound. It is very important step to avoid the aggregation of the halloysites in the coating formulation. Formation of the any aggregated nanocontainers will make defects in the coating integrity thus reducing coating barrier properties and corrosion protection performance. The halloysite should be homogeneously distributed on the coated area to protect every part of the metal (**Figure 10**). Halloysite nanotubes were loaded with the inhibitor, 2-mercaptobenzothiazole and covered by a LbL polyelectrolyte shell to improve the control over the inhibitor release.[55] Sol-gel coatings doped with halloysites demonstrated very good corrosion inhibition in long-term corrosion tests. These results are due to the favourable halloysite structure, which provides good inhibitor storage in the lumen and limits spontaneous inhibitor leakage at the small-diameter (20–50 nm) ends covered by the polyelectrolytes. Another promising approach to keep the inhibitor inside the lumen and release it in response to a pH change is by designing pH sensitive stoppers. Successful formation of stoppers for halloysites was demonstrated by exposing halloysites loaded with benzotriazole to a Cu(II) containing solution to form insoluble metal–benzotriazole complexes at the halloysite ends.[56] The release time was tuned by controlling the thickness of the stopper complexes. Further time expansion of anticorrosion agent release was achieved by the formation of stoppers with urea–formaldehyde copolymer.[57] The corrosion protection efficiency was tested on ASTM A366 steel plates in a 0.5 M NaCl solution with the study of corrosion development by microscopy inspection and paint adhesion. The best protection was found using halloysite/mercaptobenzimidazole and benzotriazole inhibitors. Stopper formation with urea–formaldehyde copolymer provided an additional increase in corrosion efficiency as a result of the longer release of inhibitors. More detailed information about the structure and properties of the halloysite nanotubes can be found in two recent, comprehensive reviews.[58]

Performance of the organic coatings with inhibitor-loaded halloysite nanotubes was also tested by industrial neutral salt-spray test (ISO 9227 standard, 5 wt% NaCl, 35°C, **Figure 11**).

Standard commercial polyepoxy coating was used as a benchmark. Corrosion inhibitor Korantin SMK, which is alkylphosphoric ester produced by BASF with the chain length of alkyls in the ester group ranging from C6 to C10 was added

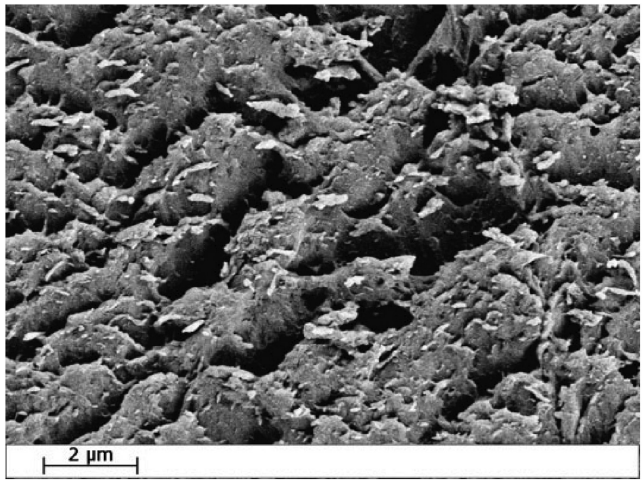

Figure 10. Distribution of inhibitor-loaded halloysite nanotubes inside sol-gel coating. Reproduced with permission.[54]

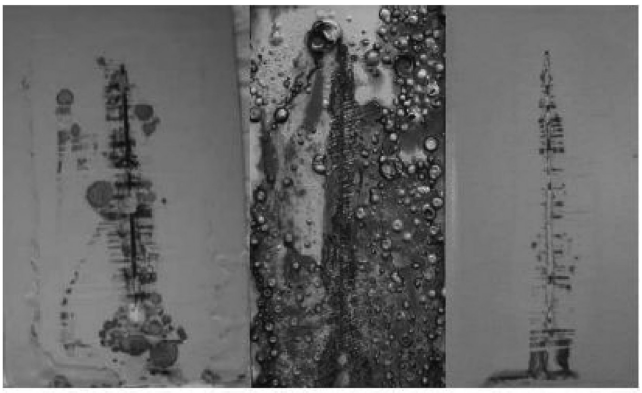

Figure 11. Neutral salt spray test results for pure polyepoxy coating (A, 1000 h), polyepoxy coating directly loaded with Korantin SMK corrosion inhibitor (B, 500 h) and polyepoxy coating in the presence of Korantin SMK loaded halloysite nanotubes (C, 1000 h).

into the coating in free form (1 wt%) and in the same amount but encapsulated into halloysite nanotubes. One can see in Figure 11, addition of free corrosion inhibitor into organic coating drastically reduces corrosion protection performance even after 500 h of the neutral salt-spray test. On the contrary, encapsulated inhibitor with controlled and sustained release ability increased corrosion protection by 5 times comparing to the pure polyepoxy coating. This is clear evidence on industrial level employing widely spread industrial test that halloysite nanotubes, loaded with industrial inhibitor, can develop new, revolutional generation of the self-healing anticorrosion coatings.

Toxicity of inorganic nanocontainers was studied using a protozoan model organism *P. caudatum*.[59] Biochemical and behavioural tests were employed to study the viability, vitality, nutrition and oxidative stress induction in ciliate protozoans. The toxicity of all nanoclays tested here is lower that of the similar size graphene oxide particles. Among analysed nanoclays, halloysite nanotubes are the most biocompatible and hence may be safely used for different industrial applications, including biomedical ones. The biosafety of the nanoparticles studied may be placed in the following order: the safest halloysite > kaolin > montmorillonite > silica > bentonite > graphene oxide. Up to 10 mg mL^{-1} of halloysite nanotubes were safe for one of the most common fresh water ciliate protist *P. caudatum*. This is 10 times more than the generally accepted safe halloysite dose for different cell cultures.

5. Conclusions & Outlook

Innovative nanocontainers of various types from sustainable materials gain more and more attention for application in various smart systems from drug delivery though bioactive surfaces to corrosion protection and further. Incorporation of different functionalities into nanocontainer shell will increase the potential of nanocontainers for multifunctional materials.

This paper aims to give concise review on the development of micro- and nanocontainers for self-healing corrosion protection coatings performed in the Department of Interfaces, Max-Planck Institute of Colloids and Interfaces in the period 2006–2012. The idea of using capsules (or, later, nanocontainers) as active component of the self-healing anticorrosion coatings came from Layer-by-Layer assembled capsules previously developed for drug delivery systems. First successful application of LbL nanocontainers for self-healing coatings was demonstrated for polyelectrolyte/inhibitor coated SiO_2 nanoparticles in 2006. Then, both organic and inorganic nanocontainers loaded with various inhibitors were developed for protection of steel and Al alloys on the lab scale.

Nowadays, the work on nanocontainers develops in two ways. First, the nanocontainers are very close to the industrial application and the main efforts are devoted to the up-scaling of nanocontainer production and performing industrial tests (salt-spray tests, etc.) for perspective self-healing coatings. Second, the know-how acquired during development of the nanocontainers for self-healing anticorrosion coatings is applied for encapsulation of other active materials into nanocontainers: biocides, bacteria, sensors phase change materials and ATP. This will lead in the future to the materials with unique properties or their combinations, for example, smart packages, paints with energy storage ability, self-controlled antifouling surfaces and others. All of this indicates the research of the intelligent nanocontainers is still a hot topic and can be applied in different areas of materials science.

Acknowledgements

The authors thank Prof. Dr. Helmuth Möhwald for his continuous support and encouragement. D.S. also thanks all his former group members in Max Planck Institute of Colloids and Interfaces for very fruitful work we did. This paper was financially supported by ERC ENERCAPSULE grant.

Received: April 15, 2016
Revised: May 24, 2016
Published online:

[1] B. J. Blaiszik, S. L. B. Kramer, S. C. Olugebefola, J. S. Moore, N. R. Sottos, S. R. White, *Annual Review of Materials Research* **2010**, *40*, 179.
[2] D. G. Shchukin, H. Möhwald, *Science* **2013**, *341*, 1458.
[3] D. G. Shchukin, D. Borisova, H. Möhwald, in *Self-Healing Polymers* (Ed.: W. Binder) Wiley-VCH, Weinheim, Germany **2013**, pp. 381–401.
[4] a) D. G. Shchukin, H. Möhwald, *SMALL* **2007**, *3*, 926; b) J. Yamuna, T. Siva, S. S. S. Kumari, S. Sathiyanarayanan, *RSC Advances* **2016**, *6*, 79.
[5] a) M. A. C. Stuart, W. T. S. Huck, J. Genzer, M. Mueller, C. Ober, M. Stamm, G. B. Sukhorukov, I. Szleifer, V. V. Tsukruk, M. Urban, F. Winnik, S. Zauscher, I. Luzinov, S. Minko, *Nature Materials* **2010**, *9*, 101; b) B. M. Bailey, Y. Leterrier, S. J. Garcia, S. van der Zwaag, V. Michaud, *Progress in Organic Coatings* **2015**, *85*, 189.
[6] a) S. R. White, N. R. Sottos, P. H. Geubelle, J. S. Moore, M. R. Kessler, S. R. Sriram, E. N. Brown, S. Viswanathan, *Nature* **2001**, *409*, 794; b) A. Rahimi, S. Amiri, *J. Polymer Research* **2016**, *4*, 1.
[7] a) C. J. Hansen, K. Wu, K. S. Toohey, N. R. Sottos, S. R. White, J. A. Lewis, *Adv. Mater.* **2009**, *21*, 4143; b) A. Yabuki, T. Shiraiwa, I. W. Fathona, *Corrosion Science* **2016**, *103*, 117.

[8] a) M. L Zheludkevich, S. K. Poznyak, L. M. Rodrigues, D. Raps, T. Hack, L. F. Dick, T. Nunes, M. G. S. Ferreira, *Corrosion Science* **2010**, *52*, 602; b) S. Hiromoto, *Corrosion Science* **2015**, *100*, 284.
[9] a) D. V. Andreeva, D. Fix, H. Möhwald, D. G. Shchukin, *Adv. Mater.* **2008**, *20*, 2789; b) F. Fan, Ch. Zhou, X. Wang, J. Szpunar, *ACS Applied Materials and Interfaces* **2015**, *7*, 27271.
[10] G. Decher, *Science* **1997**, *277*, 1232.
[11] X. Zhang, H. Chen, H. Zhang, *Chem. Commun.* **2007**, *14*, 1395.
[12] W. B. Stockton, M. F. Rubner, *Macromolecules* **1997**, *30*, 2717.
[13] M. Fang, D. M. Kaschak, A. C. Sutorik, T. E. Mallouk, *J. Am. Chem. Soc.* **1997**, *119*, 12184.
[14] A. P. R. Johnston, E. S. Read, F. Caruso, *Nano Lett.* **2005**, *5*, 953.
[15] Z. P. Wang, Z. Q. Feng, C. Y. Gao, *Chem. Mater.* **2008**, *20*, 4194.
[16] T. Lojou, P. Bianco, *Langmuir* **2004**, *20*, 748.
[17] Y. Lvov, K. Ariga, I. Ichinose, T. Kunitake, *Chem. Commun.* **1995**, *22*, 2313.
[18] C. M. Jewell, J. Zhang, N. J. Fredin, D. M. Lynn, *J. Control. Release* **2005**, *106*, 214.
[19] F. Boulmedais, V. Ball, P. Schwinte, B. Frisch, P. Schaaf, J.-C. Voegel, *Langmuir* **2003**, *19*, 440.
[20] J. Anzai, T. Hoshi, N. Nakamura, *Langmuir* **2000**, *16*, 6306.
[21] T. Serizawa, M. Yamaguchi, M. Akashi, *Macromolecules* **2002**, *35*, 8656.
[22] T. Cassier, A. Sinner, A. Offenhauser, H. Möhwald, *Colloid Surf. B* **1999**, *15*, 215.
[23] M. Dimitrova, Y. Arntz, P. Lavalle, F. Meyer, M. Wolf, C. Schuster, Y. Haikel, J. C. Voegel, J. Ogier, *Adv. Funct. Mater.* **2007**, *17*, 233.
[24] A. A. Mamedov, N. A. Kotov, M. Prato, D. M. Guldi, J. P. Wicksted, A. Hirsch, *Nat. Mater.* **2002**, *1*, 190.
[25] a) E. Donath, G. B. Sukhorukov, F. Caruso, S. A. Davis, H. Möhwald, *Angew. Chem. Int. Ed.* **1998**, *37*, 2202; b) C. S. Peyratout, L. Dahne, *Angew. Chem. Int. Ed.* **2004**, *43*, 3762.
[26] D. G. Shchukin, G. B. Sukhorukov, *Adv. Mater.* **2004**, *16*, 671.
[27] S. Moya, G. B. Sukhorukov, M. Auch, E. Donath, H. Möhwald, *J. Colloid & Interface Science*, **1999**, *216*, 297.
[28] K. Köhler, D. G. Shchukin, G. B. Sukhorukov, H. Möhwald, *J. Phys. Chem. B* **2005**, *109*, 18250.
[29] A. G. Skirtach, A. A. Antipov, D. G. Shchukin, G. B. Sukhorukov, *Langmuir* **2004**, *20*, 6988.
[30] Z. H. Lu, M. D. Prouty, Z. H. Guo, V. O. Golub, C. S. S. R. Kumar, Y. M. Lvov, *Langmuir* **2005**, *21*, 2042.
[31] D. G. Shchukin, D. A. Gorin, H. Möhwal, *Langmuir* **2006**, *22*, 7400.
[32] D. G. Shchukin, K. Köhler, H. Möhwald, *J. Am. Chem. Soc.* **2006**, *22*, 4560.
[33] T. Borodina, E. Markvicheva, S. Kunizhev, H. Möhwald, G. B. Sukhorukov, O. Kreft, *Macromol. Rapid Commun.* **2007**, *28*, 1894.
[34] D. G. Shchukin, M. Zheludkevich, K. Yasakau, S. Lamaka, M. G. S. Ferreira, H. Möhwald, *Adv. Mater.* **2006**, *18*, 1672.
[35] M. L. Zheludkevich, D. G. Shchukin, K. A. Yasakau, H. Möhwald, M. G. S. Ferreira, *Chem. Mater.* **2007**, *19*, 402.
[36] E. M. Shchukina, D. G. Shchukin, *Adv. Drug. Delivery Rev.* **2011**, *63*, 837.
[37] D. O. Grigoriev, T. Bukreeva, H. Möhwald, D. G. Shchukin, *Langmuir* **2008**, *24*, 999.
[38] a) M. F. Haase, D. Grigoriev, H. Möhwald, B. Tiersch, D. G. Shchukin, *Langmuir* **2011**, *27*, 74; b) M. F. Haase, D. O. Grigoriev, D. G. Shchukin, *Adv. Mater.* **2012**, *24*, 2429.
[39] H. Yi, Y. Yang, X. Gu, J. Huang, C. Wang, *J. Mater. Chem. A* **2015**, *3*, 13749.
[40] a) C. Suryanarayana, R. Chowdoji, D. Kumar, *Prog. Org. Coat.* **2008**, *63*, 72; b) T. Szabo, J. Telegdi, L. Nyikos, *Prog. Org. Coat.* **2015**, *84*, 136.
[41] P. D. Tatiya, R. K. Hedaoo, P. P. Mahulikar, V. V. Gite, *Industrial & Engineering Chemistry Research* **2013**, *52*, 1562.
[42] A. Latnikova, D. O. Grigoriev, J. Hartmann, H. Möhwald, D. G. Shchukin, *Soft Matter* **2011**, *7*, 369.
[43] A. Latnikova, D. O. Grigoriev, J. Hartmann, H. Möhwald, D. G. Shchukin, *Soft Matter* **2012**, *8*, 10837.
[44] Y. K. Song, C. M. Chung, *Polymer Chemistry* **2013**, *4*, 4940.
[45] a) D. Borisova, H. Möhwald, D. G. Shchukin, *ACS Nano* **2011**, *5*, 1939; b) D. Borisova, H. Möhwald, D. G. Shchukin, *ACS Applied Materials & Interfaces* **2012**, *4*, 2931; c) M. J. Hollamby, D. Borisova, H. Möhwald, D. Shchukin, *Chemical Communications* **2012**, *48*, 115.
[46] Z. Zheng, M. Schenderlein, X. Huang, N. J. Brownball, F. Blanc, D. G. Shchukin, *ACS Applied Materials & Interfaces* **2015**, *7*, 22756.
[47] B. J. Blaiszik, N. R. Sottos, S. R. White, *Compos. Sci. Technol.* **2008**, *68*, 978.
[48] X. Q. Xu, Y. H. Guo, W. P. Li, L. Q. Zhu, *Int. Journal of Minerals Metallurgy and Materials* **2011**, *18*, 377.
[49] H. Choi, K. Y. Kim, J. M. Park, *Prog. Org. Coat.* **2013**, *76*, 1316.
[50] M. J. Hollamby, D. Fix, I. Dönch, D. Borisova, H. Möhwald, D. G. Shchukin, *Adv. Mater.* **2011**, *23*, 1361.
[51] a) S. K. Samanta, M. Fritsch, U. Scherf, W. Gomulya, S. Z. Bisri, M. A. Loi, *Acc. Chem. Res.* **2014**, *47*, 2446; b) S. K. Lakkaraju, W. Hwang, *Phys. Rev. Lett.* **2009**, *102*, 118102.
[52] R. Price, B. Gaber, Y. Lvov, *Journal of Microencapsulation* **2001**, *18*, 713.
[53] E. Abdullayev, A. Joshi, W. B. Wei, Y. F. Zhao, Y. Lvov, *ACS Nano* **2012**, *6*, 7216.
[54] D. Fix, D. V. Andreeva, Y. M. Lvov, D. G. Shchukin, H. Möhwald, *Adv. Func. Mater.* **2009**, *19*, 1720.
[55] a) D. G. Shchukin, H. Möhwald, *Adv. Funct. Mater.* **2007**, *17*, 1451; b) D. G Shchukin, S. V. Lamaka, K. A. Yasakau, M. L. Zheludkevich, M. G. S. Ferreira, H. Möhwald, *J. Phys. Chem. C* **2008**, *112*, 958.
[56] E. Abdullayev, R. Price, D. Shchukin, Y. Lvov, *ACS Applied Materials & Interfaces* **2009**, *1*, 1437.
[57] A. Joshi, E. Abdullayev, A. Vasiliev, O. Volkova, Y. Lvov, *Langmuir* **2013**, *29*, 7439.
[58] a) Y. Lvov, E. Abdullayev, *Progress in Polymer Sci.* **2013**, *38*, 1690; b) Y. Lvov, W. Wang, L. Zhang, R. Fakhrullin, *Adv. Mater.* **2016**, *28*, 1227.
[59] M. Kryuchkova, A. Danilushkina, Y. Lvov, R. Fakhrullin, *Environ. Sci.: Nano* **2016**, *3*, 442.

